Appl. Phys. B 80, 399–403 (2005)
DOI: 10.1007/s00340-005-1752-2

Applied Physics B
Lasers and Optics

S.A. TRUSHIN
S. PANJA
K. KOSMA
W.E. SCHMID
W. FUß✉

Supercontinuum extending from >1000 to 250 nm, generated by focusing ten-fs laser pulses at 805 nm into Ar

Max-Planck-Institut für Quantenoptik, 85741 Garching, Germany

Received: 31 December 2004 /
Published online: 24 February 2005 •

ABSTRACT Ten femtosecond pulses at 805 nm with energy up to 1 mJ were produced by self-phase modulation of 45-fs pulses in Ar at atmospheric pressure and subsequent compression by chirped mirrors. Focusing part of this radiation again into Ar at atmospheric pressure generates a single filament with broadband emission covering the range from >1000 to 250 nm. This range extends farther into the UV than previously observed with such low energies, overlapping even the region of the third harmonic. Only a small fraction of the power is contained outside the central spot. Using a simple prism compressor, pulses were obtained with durations of 70 fs and energies of 700 nJ in the range 270–290 nm.

PACS 42.65.Jx; 42.65.Ky; 42.65.Re

1 Introduction

Propagation of an intense laser pulse in any medium results in self-phase modulation (SPM) (see, e.g., [1]). SPM is caused by the nonlinear index of refraction n_2. This is because the total index of refraction n follows the time dependence of the laser intensity $I(t)$ and the phase φ is proportional to

$$n = n_0 + n_2 I(t), \tag{1}$$

$$\varphi = kz = n(\omega/c)z, \tag{2}$$

where k is the wavenumber, z the propagation coordinate, ω the circular frequency, and c the speed of light. The phase delay is largest at the maximum of I, and this modulation of φ creates new frequencies (because $\omega = -\mathrm{d}\varphi/\mathrm{d}t$). They are shifted to the red in the rising wing of the laser pulse and to the blue in the tail, so that the resulting pulse is chirped. After some propagation in the medium, the pulse maximum is delayed versus the wings, due to the higher n. This leads to a self-steepening of the falling edge of the pulse. For this reason, the resulting broad spectrum ("supercontinuum") is usually asymmetric, extending farther to shorter wavelengths. The phase shift and frequency spread increase with z. They would even be proportional to z (Eq. 2), if self-steepening and other effects were ignored. Since pulses with a regular (e.g., temporally linear) chirp can be compressed by a prism arrangement with negative group velocity dispersion or by reflection from chirped mirrors, SPM has become a standard technique for pulse shortening (see, e.g., [2]). Typically weak pulses are spectrally broadened by SPM in solid materials. However, high-power pulses are focused into a gas for this purpose. To extend the interaction length at which the intensity remains high, it is popular to guide the wave in a gas-filled capillary [3]. After compression, pulses can be obtained with durations down to a few cycles [4].

Recently, Hauri et al. demonstrated a simple alternative to the capillary [5]: They "loosely" focused their pulses (43 fs, 0.84 mJ, 800 nm) into an Ar-filled cell, compressed the resulting spectrally broadened radiation by chirped mirrors to 10.5 fs and then repeated the process, eventually obtaining pulses of 5.7 fs duration. The necessary path length with high intensity was provided by self-guiding (filamentation). This phenomenon is due to self-focusing, which arises from the "Kerr lens" produced by the transverse refractive-index profile (intensity profile multiplied by n_2). If the laser power P is equal to the (continuous-wave) critical power

$$P_{\mathrm{crit}} = \lambda^2/2\pi n_0 n_2, \tag{3}$$

self-focusing just balances the divergence due to diffraction, so that any initial beam diameter is maintained. For Ar at atmospheric pressure ($n_2 = 1.4 \times 10^{-19}$ cm^2 W^{-1} [6]), $P_{\mathrm{crit}} = 7.3$ GW cm^{-2}. If $P > P_{\mathrm{crit}}$ holds true, self-focusing would lead to a collapse of the beam diameter; but the correspondingly higher intensities ionize the gas. The resulting free electrons (density N_e) give rise to a negative contribution Δn_e to the refractive index:

$$\Delta n_\mathrm{e} = -N_\mathrm{e} e^2/\varepsilon_0 m_\mathrm{e} \omega^2, \tag{4}$$

where e and m_e are the charge and mass of the electron, and ε_0 is the vacuum dielectric constant. The transverse N_e-profile together with the associated Δn_e has thus a defocusing effect. Over some range of laser power $P > P_{\mathrm{crit}}$, a balance between this defocusing and the self-focusing gives rise to stable self-guiding over lengths much larger than the diffraction length. Filaments as long as a few kilometers have been

✉ Fax: +49-89-32905-200, E-mail: w.fuss@mpq.mpg.de

observed and used for atmospheric monitoring, which profits from the broad continuum for recording absorptions of pollutants [7, 8]. For rather high laser powers, $P \gg P_{\mathrm{crit}}$, the beam breaks up into multiple filaments. The spot of transmitted light usually "dances" under these conditions.

The *temporal* laser profile causes a time dependence of Δn_{e} and thus contributes to SPM. The new frequencies produced by this mechanism are blue-shifted. A further source of spectral broadening, primarily to the blue side, is the moving focus; this phenomenon is due to the temporal variation of the focal length in the self-focusing mechanism. A recent issue of *Appl. Phys. B* was devoted to the supercontinuum and its applications [9]. It is worth noting that the same nonlinear susceptibility, $\chi^{(3)}$, that gives rise to n_2 is also responsible for four-wave mixing and for third-harmonic generation. The former has been used to interpret many phenomena observed with self-focusing, including also spatial variation of the spectra [10, 11]. The third harmonic of Ti-sapphire laser radiation was repeatedly observed in simple focusing into air or another gas [12–16]. Aközbek et al. pointed out that the third-harmonic pulse can co-propagate with constant phase relationship with the fundamental in the filament [15, 16]. They predicted that the third harmonic is spectrally broadened and under some conditions can merge with the white-light continuum containing the fundamental; the resulting spectrum would then be continuous from the near IR to the UV spectral range.

In this work, we demonstrate the generation of such a broad supercontinuum in a simple setup, starting from 1 mJ of Ti-sapphire laser radiation. It covers the range from $\geq$1000 to 250 nm. Previously the supercontinuum, generated from ultrashort pulses with wavelength around 800 nm, typically attained 350 nm at best, and this limit has been attributed to intensity clamping in self-focusing [17]. Only at substantially higher energies, spectra of similar width were reported: Starting from >200 mJ, a continuum reaching down to 150 nm was obtained [10, 11], and most recently a width similar to ours was found by focusing up to 10 mJ in air [18].

2 Experiment and results

The commercial laser system used (Spectra-Physics Tsunami and Spitfire) emits pulses at 805 nm with energy of 2 mJ, pulse duration of ≈45 fs (FWHM), spectral half-width of 35 nm (540 cm^{-1}) at a repetition frequency of 1 kHz. After attenuation to ≤1 mJ, the beam with an initial diameter of $3w = 16$ mm is focused by a mirror with a focal length of $f = 2$ m into a windowless cell 150 cm long, containing slowly flowing argon at ambient pressure (950 mbar). The emerging radiation is then reflected three times from chirped mirrors (Layertec, -120 fs^2). The resulting pulses have a duration of 10–11 fs, measured by an interferometric autocorrelator (Femtolasers), and a spectral half-width of 100–110 nm (1540–1700 cm^{-1}). There is no measurable energy loss in the cell. A weak luminescence is observed from the focal region from a plasma column of about 10–12 cm length (assuming a Gaussian beam, twice the Rayleigh length would be 8 cm). These results fully confirm those of Hauri et al. [5].

After the chirped-mirror compression, the IR pulse is refocused to a second windowless cell with Ar flow, this time by a mirror with $f = 1$ m and a variable diaphragm ("input iris") before the focusing mirror (Fig. 1). A supercontinuum is generated with properties mainly depending on the iris diameter. The spectrum is measured by a calibrated spectrometer (Ocean Optics) covering the range of 1000–200 nm.

If the full energy (typically 0.7 mJ, fully opened iris) of the 10-fs pulses is focused into the Ar cell, a very bright luminescing column of 5–7 cm length is observed at about 10 cm before the geometrical focus. The radiation emitted in the forward direction has a very poor pointing stability, giving rise to a dancing white spot on paper. These phenomena are probably caused by multiple filamentation. However, by steadily reducing the incident pulse energy E_{p} by closing the input iris, we show that the dancing suddenly disappears at a diameter of $d \approx 5$ mm, corresponding to $E_{\mathrm{p}} = 0.3$ mJ. Larger values of E_{p} were not further investigated. With $E_{\mathrm{p}} \leq 0.3$ mJ, the luminescing column was less bright and thinner and had a length of ≈15 cm with its center at ≈3–4 cm before the geometrical focus. Under these conditions, 96% of the incident pulse energy is recovered in the transmitted radiation.

2.1 *Spectrum of the full supercontinuum beam*

Most of the spectra were measured by integrating over the beam cross section, using an Ulbricht sphere. Figure 2 shows such a spectrum under conditions optimized such that the energy in the 300 nm region is maximal. This occurs when the iris diameter and incident energy are $d \approx 5$ mm and $E_{\mathrm{p}} = 0.26$ mJ, respectively. (A spectrum of the incident radiation is also displayed for comparison.) For an independent determination of the UV power, we cut out spectral ranges around 400, 280, and 267 nm (as shown in the figure) by reflection at four corresponding dielectric mirrors. The measured efficiencies η (energies divided by E_{p}) are also indicated and compared with those calculated from the integrated partial spectra, divided by the integrated full spectrum. The measured η are larger by a factor of two, which are probably more accurate than the calculated values.

The spectrum after the second cell extends from >1000 nm to 250 nm without any gap, but is modulated. Towards shorter wavelengths, the 805-nm

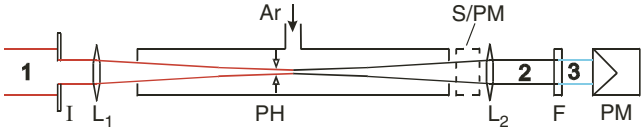

FIGURE 1 Scheme of the set-up showing the second *Ar* cell. For simplicity, the drawing shows two lenses (L_1, L_2) instead of concave mirrors (focal length $f = 1$ m) and a transmissive filter (F) instead of a set of four dielectric mirrors reflecting at the wavelengths indicated in Fig. 2. *I*: variable iris; *PH*: optional movable pinhole; *S/PM* (optional): spectrometer with integrating sphere at the entrance, or power meter; *PM*: power meter or other devices for characterizing the UV beam; *1*: incident radiation (805 nm, 0.7 mJ, 10 fs); *2*: white light emerging from the cell; *3*: UV part of the radiation. The first step (not shown) consists of a similar *Ar* cell, into which the radiation (805 nm, ≤1 mJ, 45 fs) is focused by an $f = 2$ m mirror; the emerging beam is recollimated and reflected from chirped mirrors before arriving at the iris *I*

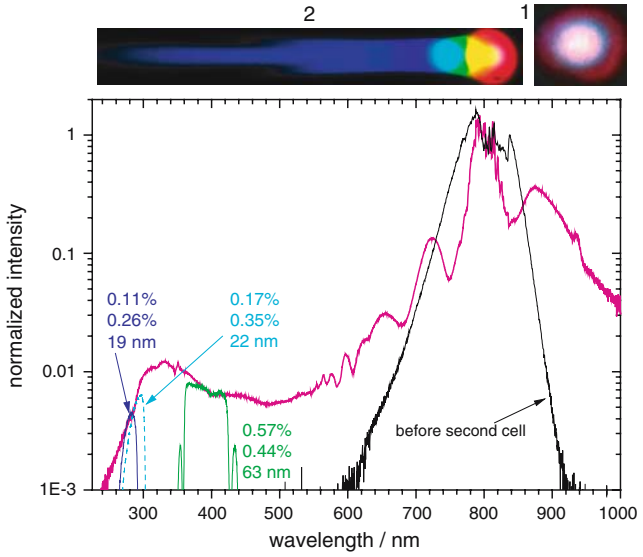

FIGURE 2 Spectrum integrated over the beam emerging from the second cell. Input energy and iris diameter were $E_p = 0.26$ mJ and $d \approx 5$ mm. The spectrum measured before the second cell is also given. Dielectric mirrors centered at 400, 290 and 267 nm were used to cut out spectral ranges as shown (halfwidths indicated). The numbers give the efficiencies (energy/total energy) as calculated from the spectrum and as measured from the reflected light, respectively. The photographs show *1* the spot after the second cell (center is overexposed), *2* the spot after dispersion by a CaF_2 prism

peak is followed by three peaks with spacing of 40 THz (1330 cm^{-1}) and some additional smaller ones. After a shallow valley, the spectrum rises again to a maximum around 320 nm. Figure 2 also displays a spectrum photographed from a white paper that was illuminated by the beam after dispersion by a CaF_2 prism. It extends over a similar wavelength range as the plotted spectrum. Obviously the beam center also contains the shortest wavelengths. Indeed the spectra vary very little over the cross section of the output beam (not shown). The non-dispersed spot has a weak red ring (14% of the energy) that is probably part of the Airy pattern caused by diffraction at the input iris.

2.2 *Varying the input iris*

As already said, opening the iris before the second cell to $d > 5$ mm (energy $E_p > 0.3$ mJ) results in a dancing output beam with only little UV light in its spectrum. This is probably due to multiple filamentation. The spectra measured as a function of the iris diameter d are shown in Fig. 3. Obviously the UV part is very sensitive for E_p and/or d. The UV fraction below 300 nm is maximal at $E_p = 0.26$–0.3 mJ; at 0.3 mJ it already shows some instability and decreases rapidly on increasing d (inset of Fig. 3; the exact shape of the $E_{UV}(d)$ curve is sensitive to the iris alignment). The spectral modulation also slightly changes on varying the iris.

2.3 *Effect of pinholes in the focal region*

We varied the diameter d_p of pinholes, placed in the center of the luminescing region (Fig. 1), from 400 to 150 μm. Their measured transmission can be well fitted by a Gaussian profile with waist w_0 over the investigated range of $w_0 \le d_p \le 3w_0$. The transmissions with $d_p = 3w_0$ and $d_p = w_0$ were 85 and 28%, respectively. Both are just 86% of the numbers calculated for a Gaussian. This is obviously due to the outer ring of the Airy pattern, caused by diffraction at the input iris. (The red ring showing up in the photograph of Fig. 2 has probably the same origin.) The fit gives a value $w_0 = 160$ μm, the same as calculated from an initial beam (iris) diameter of 5.3 mm and the focal length (1 m). Extrapolation of the Gaussian profile results in a maximum on-axis intensity of 47 TW cm^{-2}. Evaluating the UV transmissions of the pinholes in the same way results in a w_0 of 140 μm, only by 13% less than for the total radiation.

According to [15], propagation of self-focusing can be stopped by cutting the outer wings by a pinhole (400 μm in [15]; focusing conditions were similar to ours) in the filament region. In our experiment, the luminescence behind the hole was not yet visibly attenuated at 200 μm but largely suppressed at 150 μm; SPM probably soon stops after the (28% of the) radiation has passed through this pinhole. Figure 4 shows data obtained by moving it along the axis of the filament. The total energy shows a flat transmission maximum between 97

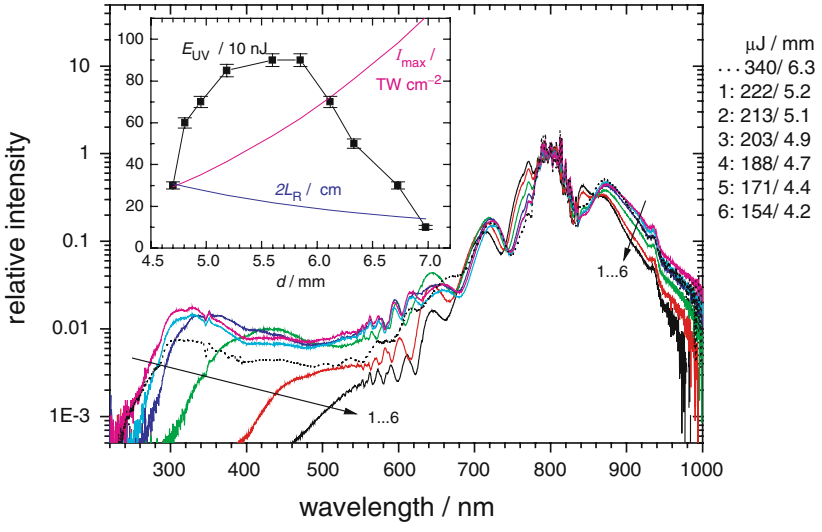

FIGURE 3 Spectra obtained on varying the diameter d of the input iris. The *solid line* spectra are labeled by 1–6. The corresponding input energies E_p (in μJ) (restricted by the iris) and the iris diameters d are listed on the right. The *inset* shows the UV energy E_{UV}, measured as reflected from four 270-nm mirrors. The curves showing the Rayleigh lengths L_R and the peak intensity I_{max} on the axis are calculated, based on the (Gaussian) beam profile measured with $d = 5.6$ mm

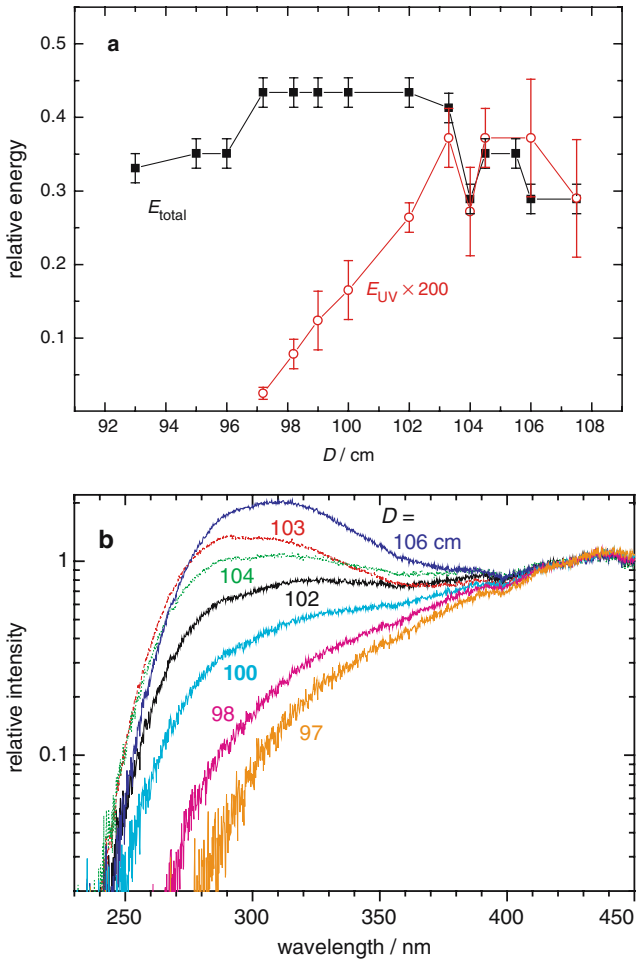

FIGURE 4 **a** Total energy E_{total} (normalized to E_{total} without pinhole) and UV energy (selected by four 270-nm mirrors) transmitted through a 150-μm pinhole versus its distance D from the focusing mirror. **b** UV spectra measured after the pinhole at these positions; they are normalized at 450 nm

and 103 cm, which obviously indicates the length of the waist. Interestingly, the UV energy, measured via the 270-nm mirror, rises till the end of the visible filament. Obviously some propagation distance z at high intensity is needed to produce the UV wavelengths. The spectra measured behind the pinhole show that on advancing along z (increasing D, the distance from the focusing mirror) the UV part is steadily growing; radiation at 290 nm is already found at 97 cm, i.e., at the beginning of the focal region.

2.4 *Pulse compression in the region of 270–290 nm*

An attempt was made to compress the pulses spectrally cut out from the UV part by dielectric mirrors with reflectivity maximum near 270 or 290 nm. This radiation was sent through a prism compressor, consisting of two Brewster-angle CaF_2 prisms combined with a mirror for reflecting the beam back through the prisms. The cross-correlation of the resulting UV pulses with the 10-fs fundamental pulse was then determined by measuring the ion yield of $Cr(CO)_6^+$ in a mass spectrometer. (The UV pulse excites a very short-lived state of $Cr(CO)_6$ [19].) After optimizing the compressor to compensate for intrinsic chirp and chirp introduced by the optical path to the detection chamber, the pulse duration was as short as 70 fs, no matter whether the width of the cut-out UV spectrum was 20 or 3.8 nm (2550 or 480 cm^{-1}). The value of 3.8 nm corresponds to a pulse that is 2.3 times the Fourier-bandwidth limit. This is presumably the limit attainable when mainly the linear chirp is compensated.

3 Discussion

To obtain a spectrum as broad as observed in this work, several prerequisites seem to be favorable: (1) few-cycle pulses, (2) a long interaction length at a high intensity, (3) a material whose n_2-value is not too small and whose ionization energy is high. The benefit of the length is shown by Eq. 2 and its derivative that is proportional to the frequency spread. Except by wave guides, one can prolong the interaction zone (a) by using long focal lengths or (b) by profiting from self-focusing and filamentation, as done in this work and in [5, 10, 11, 18] and others. Under our conditions, (a) and (b) seem to have comparable importance. This is supported by the following observations:

- The transmission of the pinholes depending on their diameter (Sect. 2.3) can be well fitted by a Gaussian, ignoring an outer ring from the Airy pattern caused by diffraction at the input iris. The Gaussian waist from the fit agrees with that calculated from diffraction optics without self-focusing.
- Transmission of the pinholes as a function of distance D from the focusing mirror showed a symmetric curve, centered at the geometric focus ($D = 102$ cm), if the cell was filled with He (which does not support self-focusing, because its n_2 is too small [10]). With Ar the curve was only slightly asymmetric (faster divergence after the focus) with a maximum of transmission at $D = 99$ cm. That is, self-focusing has shifted the focus to an only slightly smaller distance.
- If self-guiding is dominant for keeping the beam together, the spatial wings (the "reservoir" [20]) of the beam profile are focused to the axis after some propagation. Cutting this reservoir by a pinhole immediately terminates the filament [15, 21]. For example, with similar focusing but longer pulses (45 fs, 470 μJ), Aközbek et al. terminated the luminescing channel in air by a pinhole of 400 μm diameter [15]. We saw luminescence after transmission through pinholes with diameters down to 200 μm. This means that in our case only the very center of the beam is involved in self-focusing.
- The length of the luminescing column (the "filament" produced by self-focusing) was ≈12–14 cm,

which is shorter than twice the Rayleigh length $2L_R = 2\pi\omega_0^2/\lambda = 20$ cm. If self-focusing would be more dominant, it would result in channeling over a distance longer than the diffraction length $2L_R$.

The limited importance of self-focusing may have to do with the fact that our laser power (30 GW) is only by a factor of four above the critical power for Ar (7.3 GW, see Introduction section). In the first cell, it is not much less (20 GW).

Aközbek et al. predicted and observed generation of the third harmonic in air and its copropagation with the fundamental during filamentation [15, 16], which should support phase matching. They predicted separate spectral features around 270 and 800 nm, which will merge if broadening is increased [16]. Most recently, this was confirmed in the same laboratory, using higher pulse energies (≤10 mJ; pulse duration 40 fs) and a detection sensitivity of 10^{-9} as to the main peak [18]. With a sensitivity of 10^{-4} (ours was near 10^{-3}), the third harmonic would have eluded detection, and the continuum would have spread only to 300 nm. Under our conditions (≤0.3 mJ, 10 fs), there is never any isolated feature around 270 nm; also the continuing spreading of the spectrum on changing the input iris (Fig. 3) or on prolonging the interaction length (Fig. 4) is not compatible with the idea of isolated production of the third harmonic. So, the pure SPM mechanism seems do dominate under our conditions.

The main reason of our large frequency spread $\Delta\omega$ seems to be the short pulse duration. Indeed, the n_2-contribution to $\Delta\omega$ contains the derivative of the pulse shape, dI/dt (which is larger for shorter pulses), resulting from $d\varphi/dt$ (see (1) and (2) and for details [22]). Comparison with the recent work using 40-fs pulses [18] supports this view.

4 Conclusion

In a very simple set-up, we obtained a supercontinuum extending unusually far to the UV, using very modest pulse energies. There is less spatial variation of the spectrum than in previous cases. To obtain such results, it seems to be important

(1) to use few-cycle pulses (≈10 fs in our case);
(2) to extend the high-intensity interaction zone by long focal lengths f; it seems favorable when the longitudinal diffraction length is longer than the filament;
(3) to limit the laser power to a small multiple of P_{crit}.

Since $P_{crit} \propto n_2^{-1}$ and n_2 is proportional to the gas pressure p, one may hope that higher laser powers can be used, if one decreases p or uses a suitable mix of Ar with He or Ne that have a very small n_2. We also suspect that the very long focal length of $f = 5$ m was essential in obtaining the spectra extending down to 150 nm observed in [10, 11], when pulse energies of $E_p > 100$ mJ were used. With $f = 1$ m as used in our case, increasing E_p to >0.3 mJ already leads to multiple filamentation and to a reduction of the UV part.

ACKNOWLEDGEMENTS This work was supported by DFG (project FU 363/1). We appreciate very stimulating and helpful discussions with H. Schröder and S.L. Chin, and thank S.L. Chin also for providing manuscripts before publication.

REFERENCES

1 R.R. Alfano, *The Supercontinuum Laser Source* (Springer, Berlin Heidelberg New York, 1989)
2 T. Brabec, F. Krausz, Rev. Mod. Phys. **72**, 545 (2000)
3 M. Nisoli, S. De Silvestri, O. Svelto, Appl. Phys. Lett. **68**, 2793 (1996)
4 M. Nisoli, S. De Silvestri, O. Svelto, R. Szipöcs, K. Ferencz, C. Spielmann, S. Sartania, F. Krausz, Opt. Lett. **22**, 522 (1997)
5 C.P. Hauri, W. Kornelis, F.W. Helbing, A. Heinrich, A. Couairon, A. Mysyrowicz, J. Biegert, U. Keller, Appl. Phys. B **79**, 673 (2004)
6 E.T.J. Nibbering, G. Grillon, M.A. Francois, B.S. Prade, A. Mysyrowicz, J. Opt. Soc. Am. B **14**, 650 (1997)
7 G. Méjean, J. Kasparian, E. Salmon, J. Yu, J.P. Wolf, R. Bourayou, R. Sauerbrey, R. Rodriguez, L. Wöste, H. Lehmann, B. Stecklum, U. Laux, J. Eislöffel, A. Scholz, A.P. Hatzes, Appl. Phys. B **77**, 357 (2003)
8 G. Méchain, A. Couairon, Y.B. André, C. D'Amico, M. Franco, B. Prade, S. Tzortzakis, A. Mysyrowicz, R. Sauerbrey, Appl. Phys. B **79**, 379 (2004)
9 A. Zheltikov, Appl. Phys. B **77** (2003)
10 H. Nishioka, W. Odajima, K. Ueda, H. Takuma, Opt. Lett. **20**, 2505 (1995)
11 H. Nishioka, K. Ueda, Appl. Phys. B **77**, 171 (2003)
12 S. Backus, J. Peatross, Z. Zeek, A. Rundquist, M. Murnane, H.C. Kapteyn, Opt. Lett. **21**, 665 (1996)
13 J. Peatross, S. Backus, J. Zhou, M.M. Murnane, H.C. Kapteyn, J. Opt. Soc. Am. B **15**, 186 (1998)
14 A.B. Fedotov, N.I. Koroteev, M.M.T. Loy, X. Xiao, A.M. Zheltikov, Opt. Commun. **133**, 587 (1997)
15 N. Aközbek, A. Iwasaki, A. Becker, M. Scalora, S.L. Chin, C.M. Bowden, Phys. Rev. Lett. **89**, 143901.1 (2002)
16 N. Aközbek, A. Becker, M. Scalora, S.L. Chin, C.M. Bowden, Appl. Phys. B **77**, 177 (2003)
17 W. Liu, S. Petit, A. Becker, N. Aközbek, C.M. Bowden, S.L. Chin, Opt. Commun. **202**, 189 (2002)
18 F. Théberge, W. Liu, Q. Luo, S.L. Chin, Appl. Phys. B **80**, 221 (2005)
19 S.A. Trushin, W. Fuß, W.E. Schmid, Chem. Phys. **259**, 313 (2000)
20 V.P. Kandidov, O.G. Kosareva, A.A. Koltun, Quantum Electron. **33**, 69 (2003)
21 S.L. Chin, A. Brodeur, S. Petit, O.G. Kosareva, V.P. Kandidov, J. Nonlinear Opt. Phys. Mater. **8**, 121 (1999)
22 Q.Z. Wang, P.P. Ho, R.R. Alfano, in *The Supercontinuum Laser Source*, ed. by R.R. Alfano (Springer, Berlin Heidelberg New York, 1989)